Check for updates

RESEARCH ARTICLE

Co-implanting orthotopic tissue creates stroma microenvironment enhancing growth and angiogenesis of multiple tumors [version 1; referees: 1 approved, 1 approved with reservations]

Per Borgstrom[1*], Phil Oh[1,2*], Malgorzata Czarny[1,2], Brian Racine[1], Jan E Schnitzer[1,2]

[1]Sidney Kimmel Cancer Center, 10905 Road to the Cure, San Diego, CA, 92121, USA
[2]Proteogenomics Research Institute for Systems Medicine, 11107 Roselle St, San Diego, CA, 92121, USA

[*] Equal contributors

v1 **First published:** 21 May 2013, **2**:129 (doi: 10.12688/f1000research.2-129.v1)
Latest published: 29 Aug 2013, **2**:129 (doi: 10.12688/f1000research.2-129.v2)

Abstract

Tumor models are needed to study cancer. Noninvasive imaging of tumors under native conditions *in vivo* is critical but challenging. Intravital microscopy (IVM) of subcutaneous tumors provides dynamic, continuous, long-term imaging at high resolution. Although popular, subcutaneous tumor models are often criticized for being ectopic and lacking orthotopic tissue microenvironments critical for proper development. Similar IVM of orthotopic and especially spontaneous tumors is seldom possible. Here, we generate and characterize tumor models in mice for breast, lung, prostate and ovarian cancer by co-engrafting tumor spheroids with orthotopic tissue in dorsal skin window chambers for IVM. We use tumor cells and tissue, both genetically engineered to express distinct fluorescent proteins, in order to distinguish neoplastic cells from engrafted tissue. IVM of this new, two-colored model reveals classic tumor morphology with red tumor cell nests surrounded by green stromal elements. The co-implanted tissue forms the supportive stroma and vasculature of these tumors. Tumor growth and angiogenesis are more robust when tumor cells are co-implanted with orthotopic tissue versus other tissues, or in the skin alone. The orthotopic tissue promotes tumor cell mitosis over apoptosis. With time, tumor cells can adapt to new environments and ultimately even grow better in the non-orthotopic tissue over the original orthotopic tissue. These models offer a significant advance by recreating an orthotopic microenvironment in an ectopic location that is still easy to image by IVM. These “ectopic-orthotopic” models provide an exceptional way to study tumor and stroma cells in cancer, and directly show the critical importance of microenvironment in the development of multiple tumors.

Open Peer Review

Referee Status: ✓ ✓

	Invited Referees 1	2
UPDATED version 2 published 29 Aug 2013	✓	✓ report
version 1 published 21 May 2013	? report	✓ report

1 **Hong Zhao**, Methodist Hospital Research Institute USA, **Zhen Zhao**, The Methodist Hospital Research Institute USA

2 **Erik Sahai**, Cancer Research UK UK, **Danielle Park**, Cancer Research UK UK

Discuss this article

Comments (0)

Corresponding author: Jan E Schnitzer (jschnitzer@prism-sd.org)

How to cite this article: Borgstrom P, Oh P, Czarny M *et al.* **Co-implanting orthotopic tissue creates stroma microenvironment enhancing growth and angiogenesis of multiple tumors [version 1; referees: 1 approved, 1 approved with reservations]** *F1000Research* 2013, **2** :129 (doi: 10.12688/f1000research.2-129.v1)

Copyright: © 2013 Borgstrom P *et al*. This is an open access article distributed under the terms of the Creative Commons Attribution Licence, which permits unrestricted use, distribution, and reproduction in any medium, provided the original work is properly cited. Data associated with the article are available under the terms of the Creative Commons Attribution Licence, which permits unrestricted use, distribution, and reproduction in any medium, provided the original data is properly cited.

Grant information: This research was supported by grant funds (to J.E.S.) from the Komen Foundation, the state of California (TRDRP grant 18XT0196 and 20XT0161, CBCRP grant 16IB-0104, DOD CDMRP W81XWH-11-1-0693 and NIH (R01CA115215, P01CA104898, R01CA119378, and R01CA83989).
The funders had no role in study design, data collection and analysis, decision to publish, or preparation of the manuscript.

Competing interests: No relevant competing interests were disclosed.

First published: 21 May 2013, **2**:129 (doi: 10.12688/f1000research.2-129.v1)

Introduction

Relevant animal models are vital to understand the processes involved in tumor progression and to develop new therapies[1–4]. Solid tumors can be followed in their native tissue when tumor cells are administered properly into their orthotopic tissue, or when tumors are chemically induced or arise spontaneously, for instance in genetically engineered mouse models. Though *in vivo* imaging systems are advancing rapidly, imaging orthotopic tumors within the animal, especially at the cellular level for extended periods of time dynamically and continuously, remains a significant challenge. Subcutaneous models that implant rodent or human tumor cells directly into the skin of animals have quickly become the most commonly used tumor models[5–7], in part because these tumors are convenient, easy to implant, and are readily imaged outside the body[4,8].

Recent advances in intravital microscopy (IVM) have made subcutaneous tumors even easier to image dynamically at higher resolutions in live rodents through dorsal skinfold window chambers[7,9,10]. Standard light and fluorescence microscopy in this system can distinguish individual cells in the tumor so that many cellular events, such as cell migration, mitosis, pyknosis, apoptosis, and the growth of blood vessels, can be readily quantified. Intravital microscopy can also be particularly powerful for evaluating tumor imaging probes and therapeutic agents by visualizing at high resolution and quantifying tumor targeting, delivery, processing and efficacy *in vivo*, dynamically and continuously.

Tumor cell interactions with the surrounding tissue stromal environment, including extracellular matrix, local enzymes and proteases, vasculature, inflammatory cells, growth factors and hormones, can significantly affect tumor development[11–13] and are, to a large extent, extensively altered or even missing when tumors are grown in ectopic environments such as skin[14–18]. Most orthotopic tumor models and especially spontaneous tumors are not readily amenable to IVM except possibly acutely for very short periods after surgical exposure, which frequently can be quite invasive. Moreover, injecting tumor cells properly to maintain an orthotopic tissue microenvironment can be quite difficult, in part because the orthotopic organ to be injected can be so very tiny in the mouse. Making sure that all of the injected cells enter and stay inside tiny organs can be quite challenging. Microsurgical techniques with stereomicroscopic imaging can help but greatly increase the labor per mouse.

Recently, we have successfully engrafted donor tissue from healthy rat organs and mouse prostate tissue with hormonally sensitive prostate tumor cells into the dorsal skinfold of mice carrying a window chamber for dynamic and continuous IVM imaging *in vivo*[19,20]. The implanted tissue maintained both tissue and species-specificity, even expressing key organ-specific biomarkers[19]. Here, we expand this tissue transplantation and revascularization model to multiple cancers by engrafting different donor tissues with various tumor spheroids to create novel ectopic-orthotopic (EO) tumor models that permit dynamic imaging by IVM while attempting to provide and maintain an orthotopic stroma microenvironment for the tumor cells. Comparative IVM analysis of these tumors directly shows the critical incorporation of the co-engrafted tissue into the stroma of the growing tumor and ultimately the pronounced importance of this stroma and unique microenvironment for tumor growth and angiogenesis.

Methods

Materials

All materials were obtained from Sigma-Aldrich (St. Louis, MO) unless otherwise noted.

Animals

All animal experiments were performed in accordance with Institutional Animal Care and Use Commitee guidelines at Sydney Kimmel Cancer Center and Proteogenomics Research Institute for Systems Medicine. Athymic Nude-*Foxn1*^{nu}, Balb/c, C57BL/6J and FVB mice from either Charles River Laboratories (Wilmington, MA) or Jackson Laboratories (Bar Harbor, ME) GFP C57BL/6J mice were a kind gift of Dr Christa Mueller-Seiburg (Burnham Institute). Tg(TIE2GFP)287Sato/J mice were purchased from Jackson Laboratories. Female (80) and male (20) Athymic Nude-*Foxn1*^{nu}, Balb/c (5 female), C57BL/6J (10 male), GFP C57BL/6J (5 female), Tg(TIE2GFP)287Sato/J (5 female) and FVB mice (20 female) were used for the dorsal skinfold implantations and donor tissues. Once the mice were ~25g (10–14 weeks old), the chambers were placed on the dorsal skinfold and the mice were segregated into separate cages and monitored daily.

Fluorescent tumor cell lines

All cell lines were grown at 37°C in 5% CO_2 in air. N202 (gift from Joseph Lustgarten, Mayo Clinic, Scottsdale, AZ), MOVCAR-16 (gift from Denise Connolly, Fox Chase Cancer Center, Philadelphia, PA), TrampC2 (ATCC, Manassas, VA) and Lewis Lung Carcinoma (LLC-ATCC, Manassas, VA) cells were maintained in Dulbecco's Modified Eagle Medium (DMEM) high glucose supplemented with L-glutamine (2 mM), penicillin (100 U/ml), streptomycin (100 U/ml), sodium pyruvate (1 mM) (Invitrogen, Carlsbad, CA) and 10% heat-inactivated Fetal Bovine Serum (Omega Scientific, Tarzana, CA). BT474 cells (ATCC, Manassas, VA) were maintained in Hybridoma-SFM supplemented with L-glutamine (2 mM), penicillin (100 U/ml), streptomycin (100 U/ml), sodium pyruvate (1 mM) (Invitrogen, Carlsbad, CA) and 10% heat-inactivated FBS (Omega Scientific, Tarzana, CA). The histone H2B-GFP was subcloned into the SalI/HpaI sites in the LXRN vector (Clontech, Palo Alto, CA) using SalI and blunted NotI sites from the BOSH2BGFPN1 vector[21]. The mCherry vector was created from the H2B-GFP vector by cloning the mCherry gene (Dr Roger Tsien, UCSD) to replace the green fluorescent protein (GFP) gene. GP2-293 cells were infected with vesicular stomatitis virus (VSV) and the H2B-GFP or H2B-mCherry-containing virus to produce viable virus. N202, BT474, TrampC2, MOVCAR-16 and LLC cells were transduced with the viable virus to stably incorporate the H2B-GFP or H2B-mCherry gene. The transduced cells were sorted twice using fluorescence-activated cell sorting (FACs) to ensure 100% of the cells stably expressed the H2B-GFP or H2B-mCherry protein.

Tumor model

We used the classic IVM tumor model[20] with modifications. The mice, usually Athymic Nude-*Foxn1*^{nu} mice (25–30g body weight),

were anesthetized (7.3 mg ketamine hydrochloride and 2.3 mg xylazine per 100g body weight, intraperitoneal injection) and placed on a heating pad. As per the standard IVM tumor model[20,22], a titanium frame was placed onto the dorsal skinfold of the mice to sandwich the extended double layer of skin. A 15 mm diameter full-thickness circular layer of skin was then excised. The superficial fascia on top of the remaining skin was carefully removed to expose the underlying muscle and subcutaneous tissue which was then covered with another titanium frame with a glass coverslip to form the window chamber. After a recovery period of 1–2 days, tumor spheroids were implanted.

Tumor spheroids were formed by plating 50,000 cells (N202, LLC, TrampC2 and MOVCAR-16) onto 1% agar-coated 96-well non-tissue culture treated flat bottom dishes (Becton Dickinson, Franklin Lakes, NJ) (20 µl cells in 100 µl medium) and centrifuging 4 times at 1200g for 15 min, rotating the dish after every centrifugation. The cells were incubated an additional 3–7 days (depending on cell type) at 37°C in 5% CO_2 in air to form tight 3-dimensional spheroids. BT474 cells required 500,000 cells in the presence of Matrigel (BD Bioscience, San Diego) (2:1 cell volume dilution-cells to matrigel) to form spheroids in culture.

The tumor spheroids were implanted in the window chamber directly onto the exposed dorsal skin either alone to created standard, classic, subcutaneous model or with lung, liver, mammary (lactating female mammary fat pad) or prostate tissue which was excised from a donor mouse and minced into small pieces in penicillin (10,000 U/ml) – streptomycin (10,000 µg/ml) solution. One animal was usually enough to supply donor tissues for an experimental set of 15 animals except for the EO model in the case of prostate tissue when 3 animals were needed. Typically, the tumor spheroid was placed in the center of a bed of 1–2 mm of flattened minced tissue onto the subcutaneous tissue of each mouse. Tumors were allowed to re-vascularize over 7–14 days depending on model. For the BT474 cells, in some cases 10 µl of 5 mg/ml human 17β-estradiol (University of California, San Diego pharmacy) was injected subcutaneously twice weekly.

For adaptation to a new microenvironment, the tumors were allowed to re-vascularize as above. The tumor was removed and the fluorescent tumor cells were separated from non-tumor cells. New tumor spheroids were formed and re-implanted with donor mouse tissue as above. This was repeated two more times to reprogram the tumor to its new microenvironment.

Intravital microscopy (IVM) and fluorescence confocal microscopy of tumors

After implantation, tumor spheroids were allowed to revascularize (12–14 days) and tumors were imaged with intravital fluorescence video microscopy, as described[20]. The tumors were imaged with a FITC or Texas Red filter using an integrated frame grabber. Confocal microscopy was used to acquire dual fluorescence images via a Nikon E2000 microscope (20× and 60× objective lens) equipped with a Perkin Elmer UltraView 5ERS confocal system with an Hamamatsu Orca ER camera (Hamamatsu Corporation, Bridgewater, NJ). To construct movies, dual color images were taken every second; exposures for a single fluorophore were kept under 400 msec. Z-stacks were acquired every 0.5 µm and then resolved for 3D construction with Volocity LE v.3 software (Perkin Elmer).

Tumor growth

Tumors were imaged using IVM, as described above. Tumor growth was analyzed off-line from the recorded, digital, grayscale 0–to–256 images using Image-Pro Plus (Media Cybernetics, Bethesda, MD). Tumor growth was determined in two ways: by measuring the area with fluorescence signal from the GFP- or CFP-expressing tumor cells or by quantifying the cumulative fluorescence signal for the tumor over time. Tumor area was measured by counting the number of pixels with a grayscale intensity above 75, thereby making it easier to reliably follow irregularly shaped tumors. The cumulative tumor fluorescence signal was measured by signal summation of all pixels over 75. All growth curves are normalized to the tumor on day 0. In all cases, growth measured by area or aggregate fluorescence signal was found to be very similar so only one of the results is usually shown.

Mitotic and apoptotic indices

To determine mitotic and apoptotic indexes, two peripheral and two central fields (using 20x objective) from three different animals for six random fields from the growing tumor in the dorsal skinfold chamber for each tumor/tissue combination was used. Only mitotic figures in metaphase-telophase are included in the mitotic index (MI) to exclude potential artifact of nuclear membrane distortion. Apoptotic/pyknotic nuclei are defined as H2B-GFP labeled nuclei with a cross sectional area < 30 μm^2. Nuclear karyorrhexis, easily distinguishable by the vesicular nuclear condensation and brightness of H2B-GFP, is included within this apoptotic index (AI).

Vascular parameters

The vascular density of tumors was measured from digital images (obtained using 10× objective) that were "flattened" to reduce the intensity variations in the background pixels and cropped to eliminate distorted areas. The thresholding feature was used to segment the picture into objects and background. The picture was also skeletonized to measure vascular length. Vascular density was calculated as vascular length per tumor area.

Statistics

SigmaStat (Systat Software, San Jose, CA) was used to determine statistical significance. Ranked ANOVAs with the Tukey post hoc test were used and a statistically significant difference delineated if $p<0.05$.

Results and discussion

To develop new breast and lung tumor models that are amenable to continuous long-term, dynamic monitoring by IVM, yet maintain an "orthotopic" tumor microenvironment, we engrafted orthotopic tissue into the ectopic subcutaneous location, the dorsal skin with a window chamber already surgically attached, and then implanted tumor spheroids onto this donor tissue (see Methods). The tumor spheroids used in these EO tumors were formed from murine mammary adenocarcinoma (N202) and Lewis Lung Carcinoma (LLC) cells (see Methods). To follow tumor cell growth and chromosome

dynamics independent from changes in the tumor stroma and surrounding host tissue, these tumor cell lines were transduced to stably express histone H2B linked to green (GFP) or monovalent cherry (CFP) fluorescent proteins. We observed very similar growth for the parental and stably transfected fluorescent tumor cells and when tumor spheroids were implanted simultaneously with engrafted tissue or onto engrafted tissue that had already revascularized days earlier (Supplementary Figure 1a). We also assessed if the tumors implanted in syngeneic mice had a growth advantage over tumors implanted in nude mice. When we implanted syngeneic tumor cell spheroids in non-immunocompromised versus nude mice, we did not observe any noticeable differences in EO tumor growth (Supplementary Figure 1b). Both the N202 and LLC cells grew very similarly in nude mice as in FVB and C57BL/6J mice, respectively (Supplementary Figure 1b and data not shown). Consistent with this result, classic subcutaneous IVM tumor models routinely use nude mice in part because of several key advantages: i) enables implantation of a wide variety of tumor spheroids and tissues of different strains and species and ii) their abundant and hairless skin makes it easier to implant the titanium window chambers and observe the progressing tumors. Therefore, for the remaining experiments, we used fluorescent tumor spheroids implanted concurrently with other tissues in nude mice.

In the last decade or so, it has become clear that the stroma and tissue microenvironment can affect tumor development. Our ability to co-implant other tissues from normal organs with different tumor cell types in the dorsal skin window chamber provides a unique way to study the direct effects of different tissue stromas on tumor development. Moreover, this system facilitates direct imaging of the tumors over many days using IVM. To assess the effects of different tissues on the tumor growth *in vivo*, tumor spheroids were implanted directly onto the dorsal skin alone in the window chamber (as per the classic IVM subcutaneous tumor model[22]) or with different donor tissue. IVM enabled detailed visualization and quantification of tumor cell fluorescence signal as well as tumor area to assess tumor growth (see Methods). The N202 spheroids grew well on skin alone, better with each co-implanted donor tissue and most robustly with the orthotopic mammary fat pad tissue (Figure 1a and b). After 15 days, tumors grown in mammary tissue were >3 times the size of tumors grown subcutaneously. Thus, the orthotopic tissue provided the heartiest environment for tumor growth.

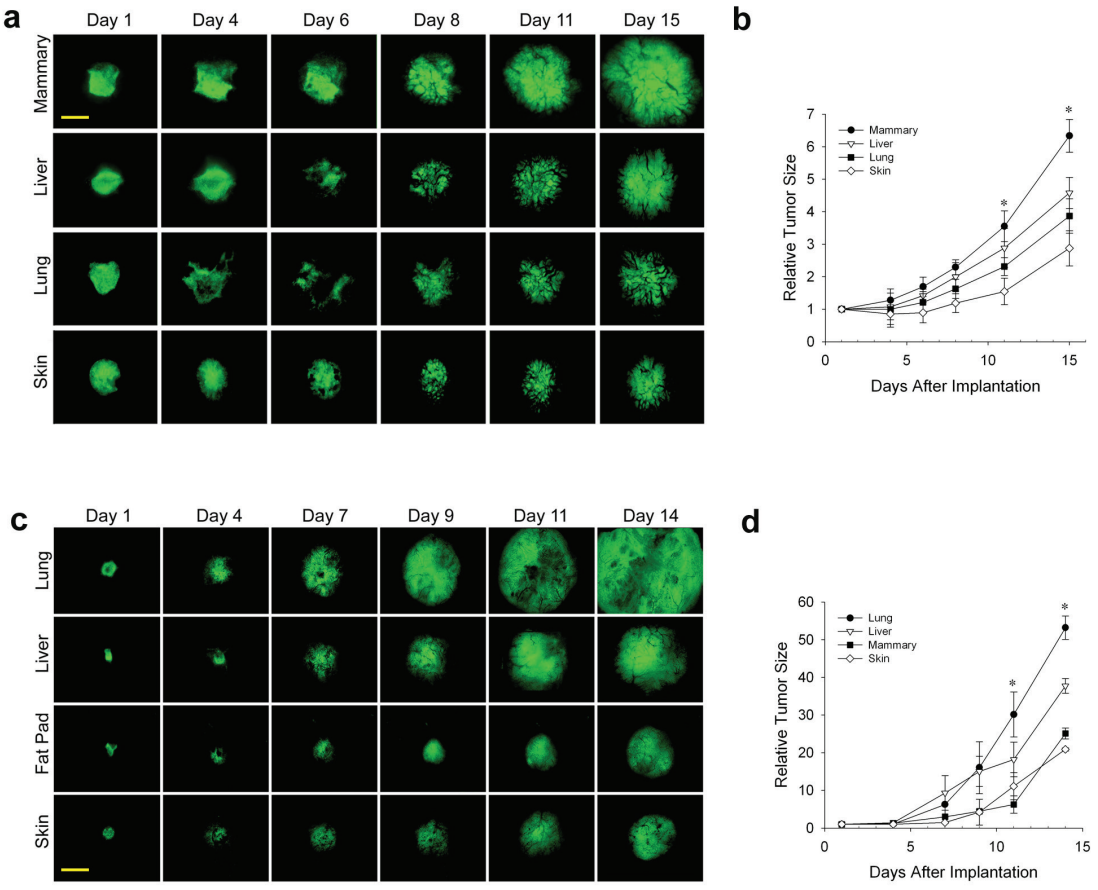

Figure 1. Effect of tissue microenvironment on tumor growth and development. (**a**–**d**) N202 (**a** and **b**) and LLC (**c** and **d**) tumor spheroids expressing H2B-GFP were implanted directly onto the dorsal skin or with mammary, liver or lung tissue as indicated and monitored through the dorsal skin window chamber by IVM at the indicated times. (**b** and **d**) Relative tumor fluorescence signal was measured by total GFP intensity relative to day 1. Scale bar = 500 μm Mean +/- SD are shown. * = p<0.05. n=3–4 mice for all experiments.

Having shown previously that prostate tumor cells grow better when implanted with prostate tissue that express key hormones required for tumor cell growth[20], we were concerned that robust growth could similarly emanate from hormones expressed in the mammary fat pad tissue. To avoid typical hormonal effects and to show that the enhanced tumor growth with co-engrafted orthotopic tissue was not restricted to one cell type, we created a new lung tumor model by implanting LLC tumor spheroids onto skin alone or co-engrafted with lung, liver, and mammary tissue (Figure 1c). Fluorescent IVM again showed the tumors growing sooner and more rapidly with orthotopic tissue. At 14 days after implantation, tumors with orthotopic tissue were again at least three times larger than subcutaneous tumors (Figure 1d). However, it should be noted for both LLC and N202 cells that after about a 10-day lag period, the growth rate of the subcutaneous tumors increased dramatically to become more similar to that of the EO tumors.

Effect of tissue microenvironment on tumor growth and development

2 Data Files

http://dx.doi.org/10.6084/m9.figshare.679762

The EO tumor model described here uses three sources of tissue, the engrafted orthotopic tissue from the donor mice, the tumor spheroids implanted onto the engrafted tissue, and the entire living host mouse. To visualize the implanted tissue cells distinctly from the neoplastic tumor cells and to determine which tissue (engrafted tissue or host tissue) gives rise to the stroma and vasculature inside the EO tumors, donor mammary tissue from GFP transgenic mice[23] was implanted simultaneously with N202 tumor spheroids expressing H2B-mCherry. Confocal fluorescence microscopy showed very typical solid tumor architecture with well-separated islands of "red" tumor cells surrounded by "green" stromal cells. When the images were projected in 3D, green vasculature with other cells derived from the orthotopic stroma could also be seen weaving amid the red tumor cells (Figure 2a–d; Supplementary Movies 1 and 2). Vascular tubes with blood flow were also readily apparent in phase images as dark vessels against the lighter stroma (Figure 2e). Under fluorescent microscopy, the blood vessels within tumors were uniformly lined with cells expressing GFP (Figure 2a, b, d and f) and were clearly distinct from tumor cells expressing mCherry (Figure 2a, b, c and g). Thus, the engrafted tissue persists to become the supportive stroma for the tumor cells in this EO model. Furthermore, these images show not only that a thriving tumor has been created with very typical, quite classic morphology but that two key components of the tumor can be marked *a priori* to be visualized distinctly in a long-term, dynamic, continuous imaging system.

To examine the vascular endothelium more specifically, we also implanted donor tissue excised from mice expressing GFP under

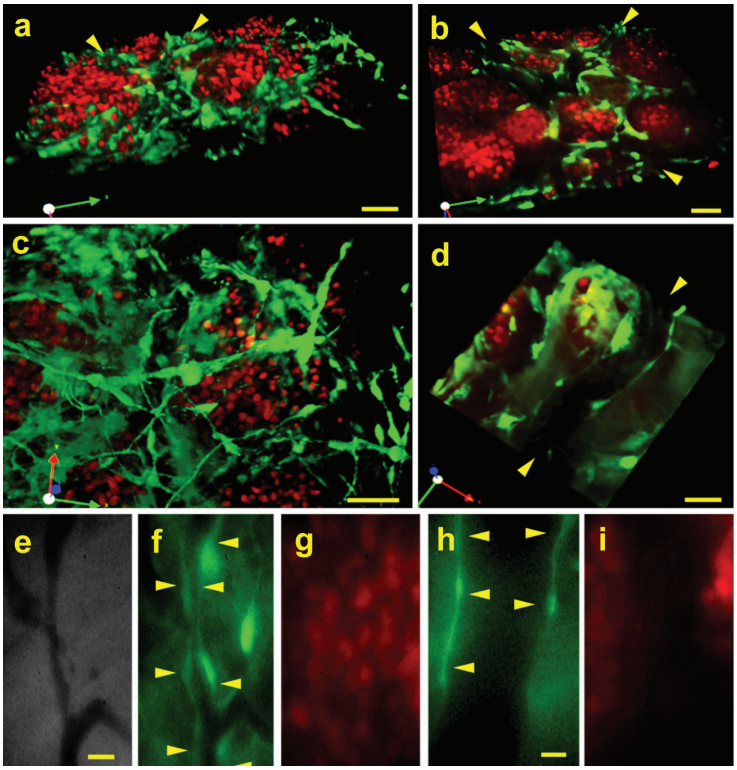

Figure 2. Distinct fluorescence imaging of tumor cells, tissue stroma and vasculature. N202 H2B-mCherry mammary tumor spheroids (red) were implanted with mammary tissue excised from a lactating GFP mouse (green) or from a mouse expressing GFP under the EC-specific TEK promoter (TEK-GFP). 20 days post-implantation, 3D confocal fluorescent microscopic images were constructed (**a–d**: GFP, **h** and **i**: TEK-GFP) as well as direct IVM fluorescent microscopic images (e-g: GFP) of the tumor and tissue stroma. Blood vessels are indicated by arrowheads. Scale bars = 10 μm (**a–d**), 20 μm (**e–g**), 5 μm (**h** and **i**).

the endothelial cell-specific promoter TEK[24]. Here again, the tumor vasculature was clearly lined with GFP-expressing endothelial cells (Figure 2h) that were clearly distinct from tumor cells (Figure 2i). The green vessels attached to host vessels lacking GFP and blood cells circulated seamlessly between the contiguous vessels. The tumor stroma and neovasculature, therefore, arose from the engrafted donor tissue and successfully revascularized by attaching to the unlabeled vessels present in the host animal.

Tumor growth ultimately requires vascular development to fulfill the metabolic demands of the cancer cells[25]. To compare the rates of revascularization, tumors growing in different tissue microenvironments were transilluminated so that dark blood vessels were readily visible against the bright tumor background (Figure 3a). The vascular development of N202 tumors grown either subcutaneously or on implanted lung tissue lagged for days behind the N202 tumors grown on orthotopic mammary tissue. Eventually, the vascular density became nearly equivalent by about 2 weeks in both models (Figure 3a and b). Blood vessels developed similarly for the LLC tumors (Figure 3c). Vascularization occurred sooner and initially was more rapid and extensive in EO tumors, likely supporting more rapid tumor growth.

Effect of tissue co-engraftment on tumor vascular development

2 Data Files

http://dx.doi.org/10.6084/m9.figshare.679764

We also tested other tumor cell lines in this system to create prostate and ovarian EO tumor models and they showed quite extreme behavior with an extraordinary dependence on co-implantation of the correct orthotopic tissue. Both Tramp-C2 prostate tumor cells (Supplementary Figure 2a) and MOVCAR-16 ovarian tumor cells (Supplementary Figure 2b) did not grow at all when implanted alone subcutaneously in the dorsal skin window chambers. They actually disappeared over a 10-day period. However, when co-implanted with their proper orthotopic tissue in the EO model, they both grew very well, with vascular development clearly evident by 6 days after implantation. Co-implantation with other ectopic tissues did not prevent tumor disappearance (data not shown). Thus, it is not just the presence of any co-implanted stroma tissue to envelop the tumor spheroid that is necessary for growth. These tumor cell lines appear actually to require the co-engraftment specifically of the orthotopic tissue to grow and to develop new blood vessels in the tumor. The orthotopic tissue co-implantation can essentially rescue *in vivo* growth and enable tumor cell lines to create a more robust and potentially useful tumor model *in vivo*.

We also observed that human tumor cells can also exhibit a strong preference for orthotopic tissue co-implantation. We implanted the well-known human breast cancer cell line BT474 as tumor spheroids in the dorsal skin window chamber with and without mouse mammary tissue. First, we did so without supplementing the mice with human estrogen, which is customary for these tumor cells. Figure 4a and b show that the tumors did not grow well and substantially regressed from the original tumor spheroid, especially

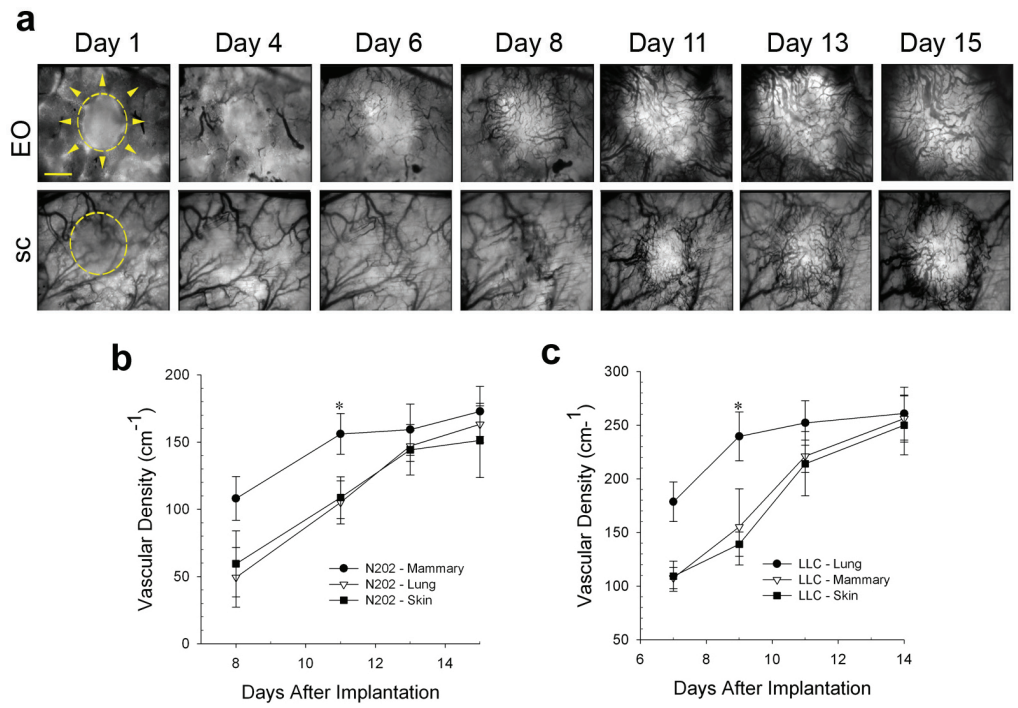

Figure 3. Effect of tissue co-engraftment on tumor vascular development. (**a**) Phase images of N202 tumor spheroids expressing H2B-GFP that were implanted directly onto the dorsal skin (sc) or with donor mammary tissue (EO) as indicated and monitored by IVM at the indicate times after implantation. N202 (**b**) and LLC (**c**) tumor vascular densities were measured at the indicated times. Scale bar = 10 μm Mean +/- SD are shown. * = p<0.05. n=3–4 mice for all experiments.

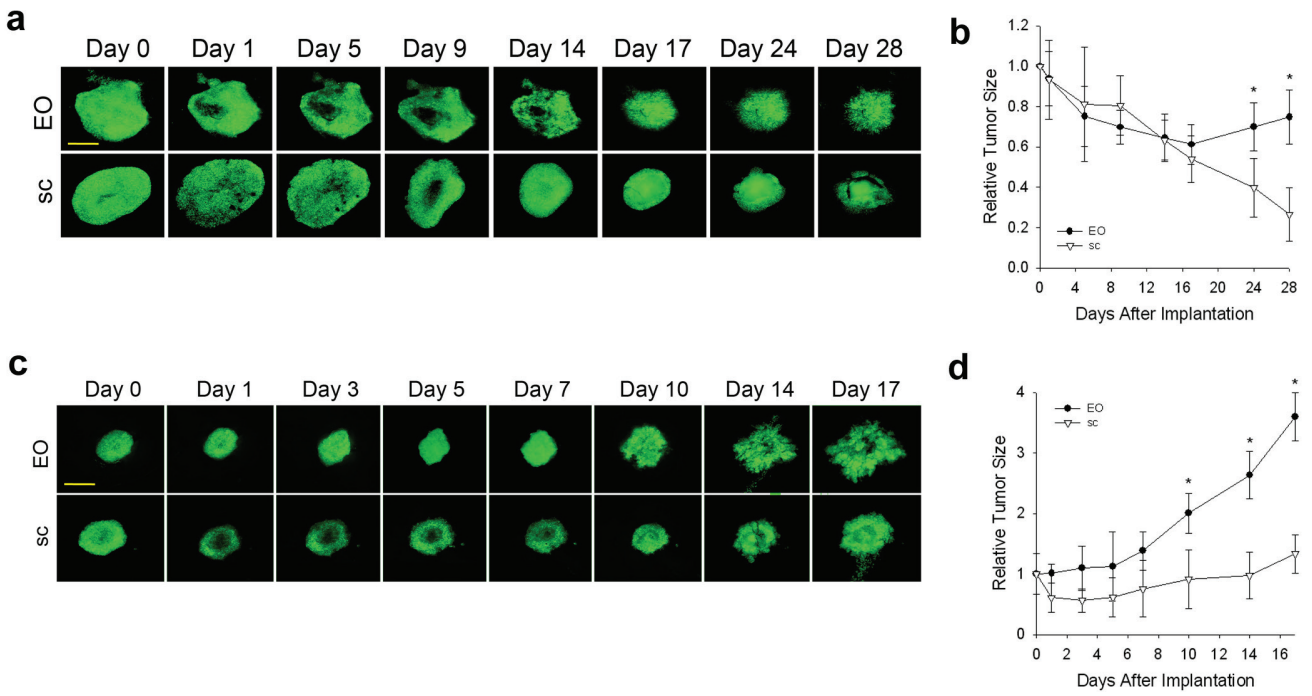

Figure 4. Effect of mouse orthotopic tissue co-engraftment on human BT474 tumor growth. BT474 tumor spheroids expressing H2B-GFP were implanted directly onto the dorsal skin (sc) (**a** and **b**) or with mouse mammary fat pad donor tissue (EO) (**c** and **d**) and monitored by IVM. (**a** and **c**) Fluorescence IVM images on the indicated days after implantation. (**b** and **d**) Tumor growth measured by fluorescence signal over time. Mice received human estrogen supplement in **c** and **d** but not **a** and **b**. Scale bar = 500 μm Mean +/- SD are shown. * = p<0.05. n=3–4 mice for all experiments.

in the subcutaneous-only implants. However, with mammary tissue, the tumor regression was reversed after 2 weeks with modest growth thereafter. When we performed the implantations this time with estrogen supplementation, tumor growth was much more robust. Figure 4c and d show that, again, the fluorescent tumors grew more quickly in the EO model than subcutaneous model. The tumor spheroids decreased in size initially in the subcutaneous model for about 1 week and then grew modestly thereafter. The EO tumors did not regress and required about 5–7 days to begin robust growth. Angiogenesis was readily evident by 8–10 days after implantation. Vascular development lagged along with little tumor growth in the subcutaneous tumors alone until after 2 weeks. Thus, it appears that human tumor cells can also benefit from orthotopic mouse tissue implantation quite similarly to the mouse tumor cell lines. Even without human estrogen supplementation, these tumors cells did better in the orthotopic stroma milieu (Figure 4a and b). Then, also with human estrogen, the tumors grew much better when exposed to an orthotopic tissue environment. Our new IVM study of multiple tumor types subjected to tissue co-implantation clearly shows that the tissue stroma can have a very significant and even dramatic effect on tumor growth and vascular development. Ultimately, every tumor type tested grew best when co-implanted with respective orthotopic tissue.

Effect of mouse orthotopic tissue co-engraftment on human BT474 tumor growth

2 Data Files

http://dx.doi.org/10.6084/m9.figshare.679765

Using IVM with the H2BGFP-labeled tumor cells allowed us to visualize directly the growing tumor cells and their fluorescent nuclei in real time. To begin to examine the cellular mechanisms mediating growth differences in the distinct tissue microenvironments, chromatin dynamics were imaged to quantify both mitotic and apoptotic cells in the LLC spheroids implanted with lung tissue, ectopically with other tissues, or subcutaneously, directly on skin (Figure 5a). The ratio of mitotic to apoptotic tumor cells in each tumor revealed that the LLC tumors growing on orthotopic tissue had a strong bias towards mitosis (Figure 5b). LLC tumors growing in mammary tissue, liver or skin had a more balanced ratio of mitosis to apoptosis. The N202 tumors showed very similar results whereas the TRAMP-C2 and MOVCAR-16 tumors also exhibited ample mitosis in the EO model, but no mitosis and ample apoptosis and cell death, as they disappeared when implanted alone subcutaneously (Supplementary Figure 2). Thus, the orthotopic tissue could create for multiple tumor cell lines a local tissue microenvironment that favored tumor growth by promoting tumor-cell mitosis over apoptosis.

Effect of tissue co-engraftment on mitotic/apoptotic indices of tumor cells

1 Data File

http://dx.doi.org/10.6084/m9.figshare.679766

In humans, tumors are not restricted to one organ, but instead eventually reprogram to alter their phenotype often in order to metastasize

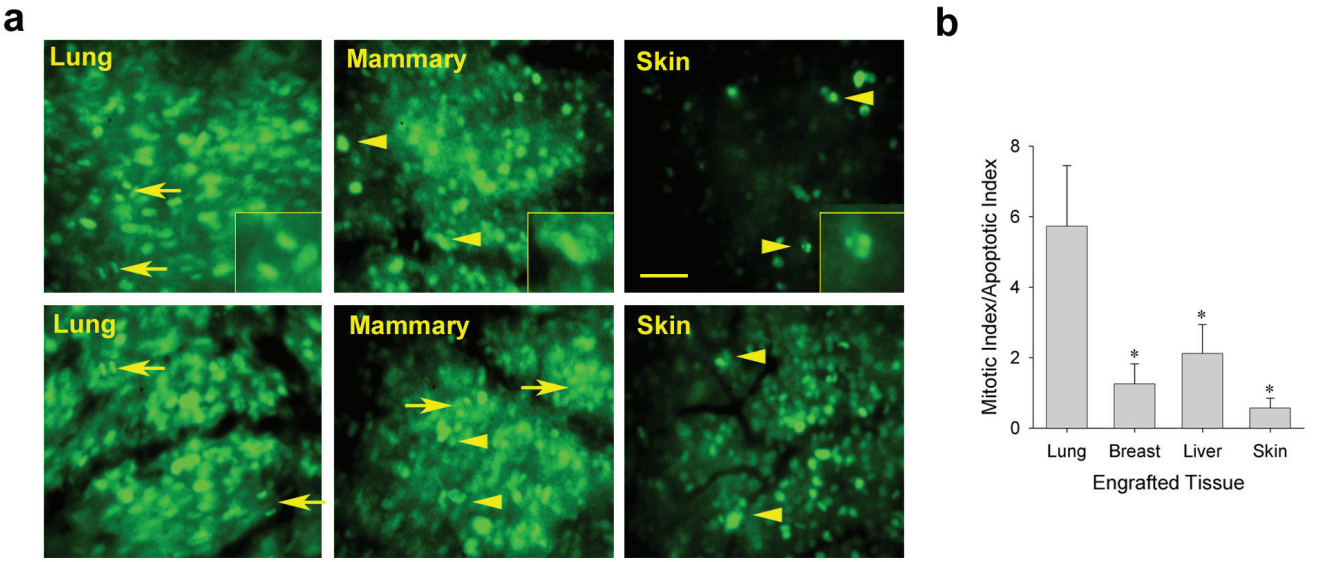

Figure 5. Effect of tissue co-engraftment on mitotic/apoptotic indices of tumor cells. (**a**) Higher magnification fluorescence micrographs showing LLC tumor cells growing in indicated tissues (9 days post-implantation) to assess their effect on relative tumor cell mitosis and apoptosis. Mitotic (arrows) and apoptotic (arrowheads) cells were counted to determine the ratio of mitotic cells to apoptotic cells (**b**). Scale bar = 100 μm Mean +/- SD are shown. * = p<05. n=3–4 mice for all experiments.

to other organs. This well-known characteristic of cancer suggests tumor cells have the inherent ability to genetically adapt and maybe even to grow optimally in other non-orthotopic tissue environments. To determine the ability of tumor spheroids to adapt to different tissue microenvironments, we passaged N202 mammary tumor spheroids on donor lung tissue in the dorsal window chamber model (as described in the methods). Initially, mammary tumors grew poorly (Figure 6a and b) and revascularized more slowly (Figure 6c) when grown on lung tissue than orthotopic mammary tissue. However, after three passages of growing in lung tissue implanted in the IVM chamber followed by isolating and re-culturing the tumor cells for spheroid formation and then re-implantation, mammary tumor cells eventually grew much more robustly and revascularized faster (Figure 6a–c) on donor lung tissue. Remarkably, when lung-adapted mammary tumor cells were implanted onto mammary tissue, the tumors grew quite poorly and revascularized rather slowly (Figure 6a–c). In fact, their growth and revascularization was similar to the growth on the lung tissue prior to being trained via lung tissue passaging. Thus, interactions between tumor cells and stroma become evident, including tumor cells adapting to a new tissue microenvironment and eventually reaching a new phenotype optimized for the new stroma, but no longer flourishing in the original orthotopic tissue.

Tumor cell adaptation to non-orthotopic tumor microenvironment

2 Data Files

http://dx.doi.org/10.6084/m9.figshare.679767

IVM offers an unparalleled view into tumor development, allowing dynamic, high resolution, *in vivo* imaging of molecular and cellular events. Here, we greatly expand the relevancy of the classic IVM tumor model by introducing orthotopic tissue into the dorsal skinfold chambers, thereby creating EO tumor models allowing easy and direct manipulation of the tissue microenvironment that can now be viewed with a long-term, dynamic, continuous imaging system. We show that tumors in an orthotopic tissue microenvironment grow more robustly and develop vasculature more rapidly than subcutaneous and other ectopic tissue models. The orthotopic environment facilitates tumor cell mitosis over apoptosis. As new blood vessels are needed to support tumor growth, the faster growing blood supply observed in the EO models likely supports the greater rates of mitosis in the tumor cells growing with orthotopic tissue versus just subcutaneously. Recreating the orthotopic tumor microenvironment in the dorsal skinfold window chamber is a significant advancement that maintains the power of the IVM imaging system. This approach incorporates the more relevant orthotopic tissue microenvironment, while still being amenable to dynamic imaging by IVM. The IVM experiments show improvements over subcutaneous tumor models and provide key direct evidence that the tumor stroma and microenvironment can dramatically influence growth and angiogenesis.

Though tumor models abound, one of the many strengths of this novel EO model is its ease of use. True orthotopic tumor models, in which tumors are implanted onto orthotopic tissue, can be technically difficult to create. For example, it is quite challenging to inject mammary tumor cells into the very tiny mammary tissue of

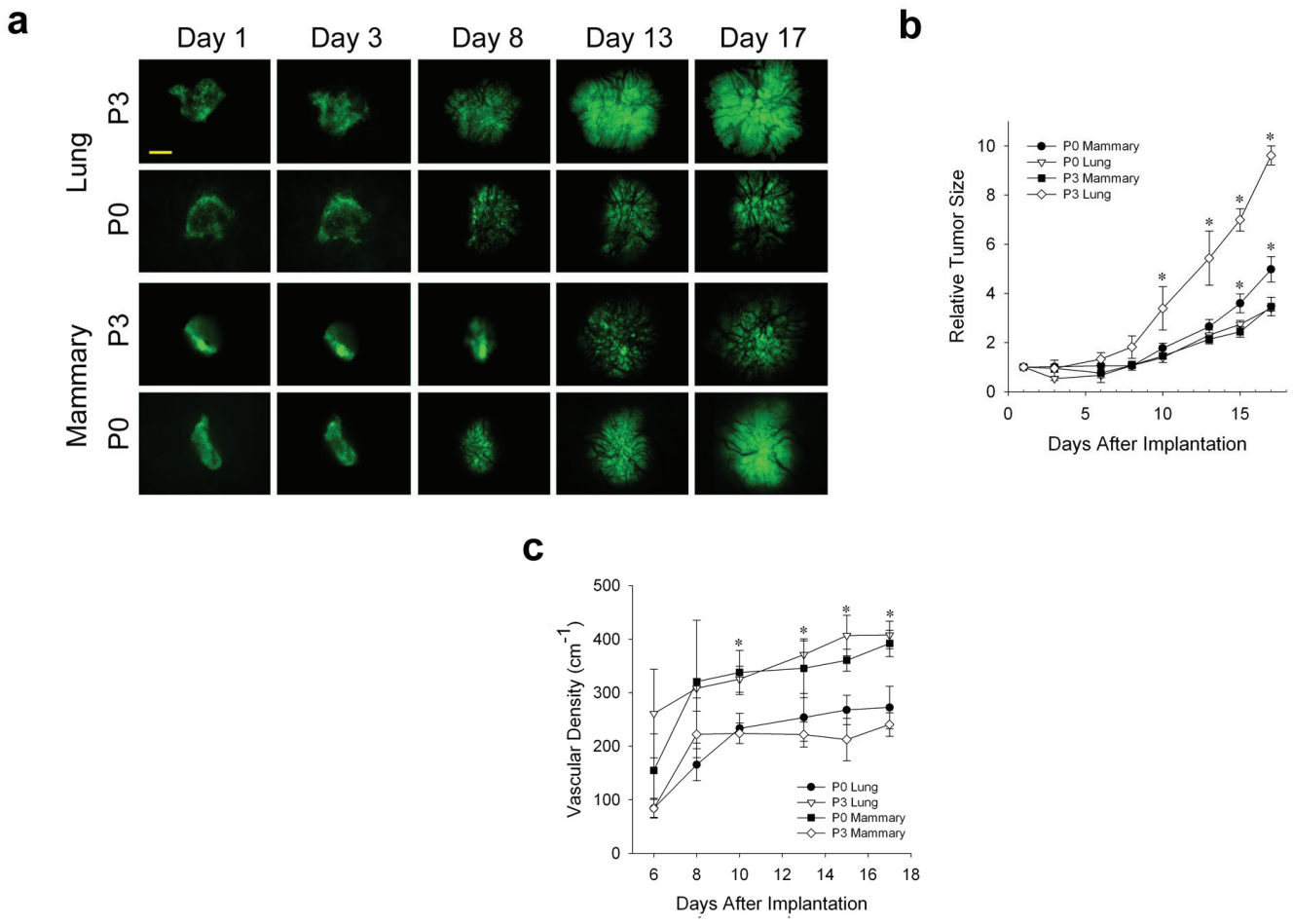

Figure 6. Tumor cell adaptation to non-orthotopic tumor microenvironment. (**a**) N202 tumor spheroids were passaged 0 or 3 times on lung tissue, as described in methods, and implanted onto engrafted lung or fat pad tissue and monitored by IVM at the indicated times. (**b**) Tumor size was measured by total tumor area relative to day 1. (**c**) Tumor vascular density of the indicated passaged N202 tumor spheroid was also determined as described in the methods. Scale bar = 500 μm Mean +/- SD are shown. * = $p<0.05$. n=3–4 mice for all experiments.

the mouse, especially when the cell number or injection volume is similar to that of mouse tissue. Genetic tumor models are complicated and costly to create and are specialized for a very specific set of genetic defects. Dynamic *in vivo* imaging, especially at the cellular level, is also very limited in many of these models. The EO model overcomes each of these difficulties. Engrafting tissue in the dorsal skinfold chamber is fairly straightforward. Numerous types of tumors and donor orthotopic tissue can be readily implanted. This model is widely applicable to many tumor types and is amenable to dynamic imaging by IVM, which offers an unparalleled view into tumor development, allowing dynamic, high resolution, *in vivo* imaging of molecular and cellular events.

Importantly, recreating the orthotopic tumor microenvironment in the dorsal skinfold window chamber allows researchers to focus on tumor-stroma interactions in a more controlled environment. Growing tumor spheroids in different microenvironments revealed that tumors in an orthotopic tissue microenvironment grow more robustly than subcutaneous and other ectopic tissue models. The orthotopic environment facilitates tumor cell mitosis over apoptosis. As new blood vessels are needed to support tumor growth, this faster growing blood supply likely supports greater rates of tumor-cell mitosis in tumor cells growing orthotopically versus subcutaneously. However, growth in a single microenvironment is not hardwired into the tumor cell. Tumor cells clearly have the ability to adapt to new microenvironments. Thus, these new tumor models may allow the ongoing interaction between tumor and stroma to be examined in greater detail and with more precise control than previously possible. Further experimentation comparing EO versus subcutaneous tumors may be warranted. Such studies may find additional functional and molecular distinctions that not only uncover stroma effects, but also provide contrasts to actual tumors in humans.

Author contributions

All authors contributed to the planning and execution of experiments. PO, PB and BR performed the IVM experiments and MC performed the confocal experiments.

Competing interests

No relevant competing interests were disclosed.

Grant information

This research was supported by grant funds (to J.E.S.) from the Komen Foundation, the state of California (TRDRP grant 18XT0196 and 20XT0161, CBCRP grant 16IB-0104, DOD CDMRP W81XWH-11-1-0693 and NIH (R01CA115215, P01CA104898, R01CA119378, and R01CA83989).

The funders had no role in study design, data collection and analysis, decision to publish, or preparation of the manuscript.

Acknowledgments

We thank Jamie Huberman and Dale Winger for technical assistance and Kerri Massey for help with manuscript preparation. We would like to thank Dr Roger Tsien for the gift of the mCherry construct, Dr Denise Connolly for the gift of the MOVCAR-16 cells and Dr Joseph Lustgarden for the gift of the N202 cells.

Supplematary materials

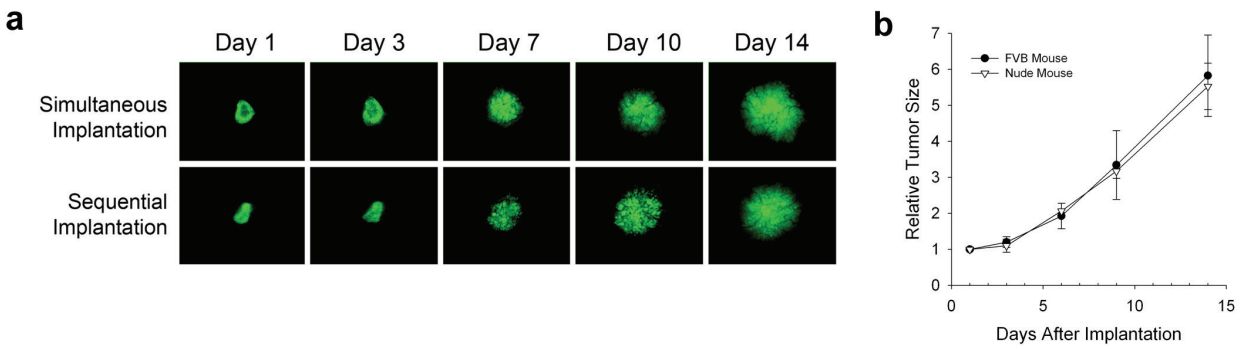

Supplementary Figure 1. Effect of tissue co-engraftment on tumor development. (**a**) Comparison of simultaneous and sequential implantation. N202 tumor spheroids expressing H2B-GFP were implanted either simultaneously with the donor tissue or after the donor tissue was implanted and allowed to revascularize. The days represent the time the tumor spheroids were allowed to grow after they were implanted. As observed, the growth and vascularity of the tumors are very similar between simultaneous and sequential implantation. (**b**) Comparison of the relative tumor size of ectopic/orthotopic implantation of tumor spheroids in FVB versus nude mice. N202 tumor spheroids expressing H2B-GFP were implanted in FVB or nude mice with the donor mammary fat pad tissue, allowed to revascularize, and imaged by IVM to measure tumor size by total fluorescence signal on the indicated day post tumor implantation. Again, the growth of the tumors are observed to be very similar.

Effect of tissue co-engraftment on tumor development

1 Data File

http://dx.doi.org/10.6084/m9.figshare.679768

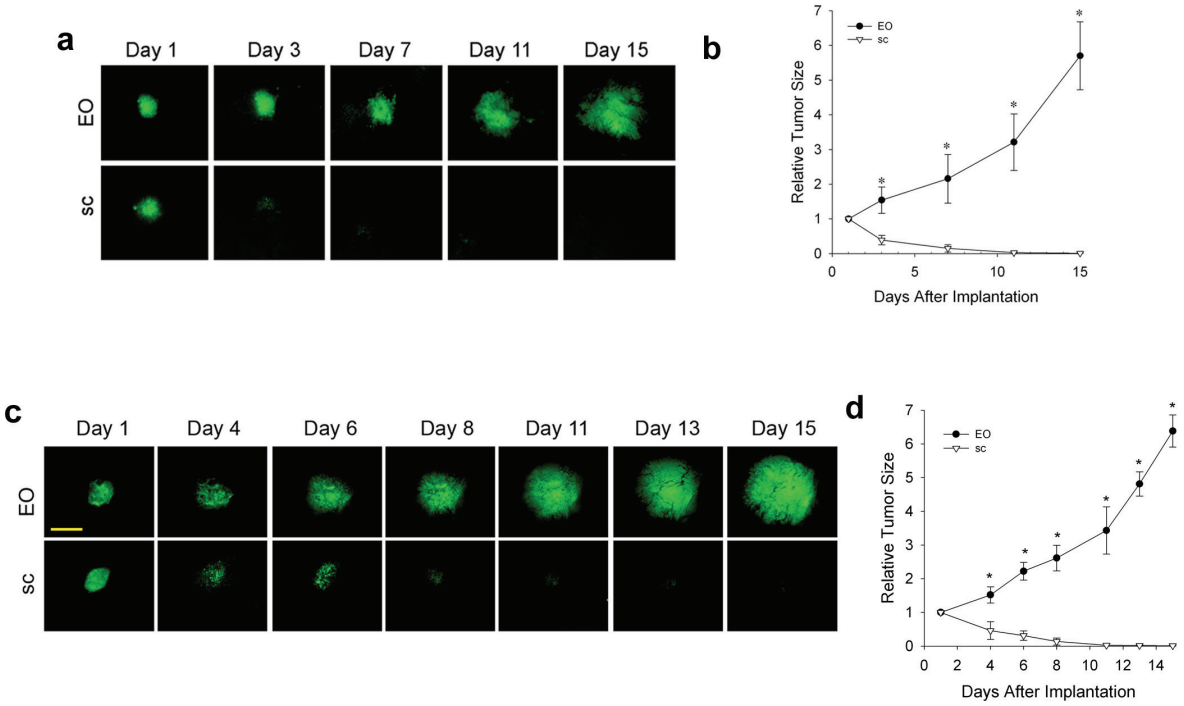

Supplementary Figure 2. Effect of orthotopic tissue co-implantation on TRAMP C2 and MOVCAR16 tumor growth. Fluorescence images (**a** and **c**) and growth curves (**b** and **d**) of TRAMPC2 (**a** and **b**) and MOVCAR-16 (**c** and **d**) tumor spheroids expressing H2B-GFP that were implanted directly onto the dorsal skin (sc) or with respective orthotopic donor tissue (EO) (prostate and ovary respectively) and monitored through the dorsal skin window chamber by IVM at the indicated times. Scale bar = 500 µm Mean +/- SD are shown. * = p<0.05. n=3–4 mice for all experiments.

Effect of orthotopic tissue co-implantation on TRAMP C2 and MOVCAR16 tumor growth

2 Data Files

http://dx.doi.org/10.6084/m9.figshare.679769

Supplementary Movies S1 and S2. Distinct imaging of tumor cells, tissue stroma and vasculature

2 Movie Files

http://dx.doi.org/10.6084/m9.figshare.679831

References

1. DeVita VT Jr, Chu E: **A history of cancer chemotherapy.** *Cancer Res.* 2008; **68**(21): 8643–53.
PubMed Abstract | Publisher Full Text
2. Suggitt M, Bibby MC: **50 years of preclinical anticancer drug screening: empirical to target-driven approaches.** *Clin Cancer Res.* 2005; **11**(3): 971–81.
PubMed Abstract
3. Ellis LM, Hicklin DJ: **VEGF-targeted therapy: mechanisms of anti-tumour activity.** *Nat Rev Cancer.* 2008; **8**(8): 579–91.
PubMed Abstract | Publisher Full Text
4. Kerbel RS: **Human tumor xenografts as predictive preclinical models for anticancer drug activity in humans: better than commonly perceived-but they can be improved.** *Cancer Biol Ther.* 2003; **2**(4 Suppl 1): S134–9.
PubMed Abstract
5. Jain RK, Munn LL, Fukumura D: **Dissecting tumour pathophysiology using intravital microscopy.** *Nat Rev Cancer.* 2002; **2**(4): 266–76.
PubMed Abstract | Publisher Full Text
6. Tozer GM, Ameer-Beg SM, Baker J, *et al.*: **Intravital imaging of tumour vascular networks using multi-photon fluorescence microscopy.** *Adv Drug Deliv Rev.* 2005; **57**(1): 135–52.
PubMed Abstract | Publisher Full Text
7. Vajkoczy P, Ullrich A, Menger MD: **Intravital fluorescence videomicroscopy to study tumor angiogenesis and microcirculation.** *Neoplasia (New York, N.Y.).* 2000; **2**(1–2): 53–61.
PubMed Abstract | Publisher Full Text | Free Full Text
8. Staquet MJ, Byar DP, Green SB, *et al.*: **Clinical predictivity of transplantable tumor systems in the selection of new drugs for solid tumors: rationale for a three-stage strategy.** *Cancer Treat Rep.* 1983; **67**(9): 753–65.
PubMed Abstract
9. Endrich B, Asaishi K, Gotz A, *et al.*: **Technical report--a new chamber technique for microvascular studies in unanesthetized hamsters.** *Res Exp Med (Berl).* 1980; **177**(2): 125–34.
PubMed Abstract | Publisher Full Text
10. Asaishi K, Endrich B, Gotz A, *et al.*: **Quantitative analysis of microvascular structure and function in the amelanotic melanoma A-Mel-3.** *Cancer Res.* 1981; **41**(5): 1898–904.
PubMed Abstract

11. Cano P, Godoy A, Escamilla R, *et al.*: **Stromal-epithelial cell interactions and androgen receptor-coregulator recruitment is altered in the tissue microenvironment of prostate cancer.** *Cancer Res.* 2007; **67**(2): 511–9.
PubMed Abstract | Publisher Full Text

12. Chrenek MA, Wong P, Weaver VM: **Tumour-stromal interactions. Integrins and cell adhesions as modulators of mammary cell survival and transformation.** *Breast Cancer Res.* 2001; **3**(4): 224–9.
PubMed Abstract | Publisher Full Text | Free Full Text

13. Schmeichel KL, Weaver VM, Bissell MJ: **Structural cues from the tissue microenvironment are essential determinants of the human mammary epithelial cell phenotype.** *J Mammary Gland Biol Neoplasia.* 1998; **3**(2): 201–13.
PubMed Abstract | Publisher Full Text | Free Full Text

14. Talmadge JE, Singh RK, Fidler IJ, *et al.*: **Murine models to evaluate novel and conventional therapeutic strategies for cancer.** *Am J Pathol.* 2007; **170**(3): 793–804.
PubMed Abstract | Publisher Full Text | Free Full Text

15. Killion JJ, Radinsky R, Fidler IJ: **Orthotopic models are necessary to predict therapy of transplantable tumors in mice.** *Cancer Metastasis Rev.* 1998-1999; **17**(3): 279–84.
PubMed Abstract | Publisher Full Text

16. Myers JN, Holsinger FC, Jasser SA, *et al.*: **An orthotopic nude mouse model of oral tongue squamous cell carcinoma.** *Clin Cancer Res.* 2002; **8**(1): 293–8.
PubMed Abstract

17. Nakamura T, Fidler IJ, Coombes KR: **Gene expression profile of metastatic human pancreatic cancer cells depends on the organ microenvironment.** *Cancer Res.* 2007; **67**(1): 139–48.
PubMed Abstract | Publisher Full Text

18. Onn A, Isobe T, Itasaka S, *et al.*: **Development of an orthotopic model to study the biology and therapy of primary human lung cancer in nude mice.** *Clin Cancer Res.* 2003; **9**(15): 5532–9.
PubMed Abstract

19. Oh P, Borgstrom P, Witkiewicz H, *et al.*: **Live dynamic imaging of caveolae pumping targeted antibody rapidly and specifically across endothelium in the lung.** *Nat Biotechnol.* 2007; **25**(3): 327–337.
PubMed Abstract | Publisher Full Text | Free Full Text

20. Frost GI, Lustgarten J, Dudouet B, *et al.*: **Novel syngeneic pseudo-orthotopic prostate cancer model: vascular, mitotic and apoptotic responses to castration.** *Microvasc Res.* 2005; **69**(1–2): 1–9.
PubMed Abstract | Publisher Full Text

21. Kanda T, Sullivan KF, Wahl GM: **Histone-GFP fusion protein enables sensitive analysis of chromosome dynamics in living mammalian cells.** *Curr Biol.* 1998; **8**(7): 377–85.
PubMed Abstract | Publisher Full Text

22. Lehr HA, Leunig M, Menger MD, *et al.*: **Dorsal skinfold chamber technique for intravital microscopy in nude mice.** *Am J Pathol.* 1993; **143**(4): 1055–62.
PubMed Abstract | Free Full Text

23. Okabe M, Ikawa M, Kominami K, *et al.*: **'Green mice' as a source of ubiquitous green cells.** *FEBS lett.* 1997; **407**(3): 313–9.
PubMed Abstract | Publisher Full Text

24. Motoike T, Loughna S, Perens E, *et al.*: **Universal GFP reporter for the study of vascular development.** *Genesis.* 2000; **28**(2): 75–81.
PubMed Abstract | Publisher Full Text

25. Folkman J: **Proceedings: Tumor angiogenesis factor.** *Cancer Res.* 1974; **34**(8): 2109–13.
PubMed Abstract

Open Peer Review

Current Referee Status: ? ✓

Version 1

Referee Report 27 June 2013

doi:10.5256/f1000research.1275.r1031

✓ **Erik Sahai**[1], **Danielle Park**[2]

[1] Tumour Cell Biology Laboratory, Cancer Research UK, London, UK

[2] Cancer Research UK, London, UK

This study expands on long-standing observations that tumor xenografts behave differently in different anatomical locations. The hypothesis is that there are some paracrine interactions that favour tumorigenecity that can only occur with cells or matrix from the appropriate tissue location. Many studies have suggested this over the past twenty five years, for example Nakamura *et al.* (2007), Killion *et al.* (1999), Fidler et al. (1990). This study revisits the theory in a methodical manner. Tumor cell lines from different anatomical locations are grafted with or without normal tissue from the same organ. Lung, ovarian and breast cancer cells are found to grow quicker when co-implanted with normal tissue from the lung and breast, respectively. In general, the work is thorough and convincing, although there is some scope for improvement and clarification.

Technical comments

1. Borgstrom *et al.*, use area of fluorescence signal and/or cumulative fluorescence signal as a measure of tumour size and growth (Figures 1a-d, 4a-d, and 6 a-b and Supplementary 1 a-b and 2a-d). Fluorescent signal will be attenuated at increasing depths, particularly when using low wavelength/low penetrance fluorophores such as GFP. This method is then inappropriate for irregularly shaped tumours that grow into the body of the mouse rather than just expanding along the plane of the window. In such instances tumour size will be underestimated. Ex-vivo analysis of tumour size/weight may have been more accurate.

2. Borgstrom *et al.*, define apoptotic cells by the size of the nucleus (upper cut off of $<30\mu m^2$). Is the same threshold used for all cells lines? If so, is this appropriate? When measuring karyorrhexis is each nuclear fragment counted as one apoptotic cell? As tumour cells lack a cell membrane marker, it is impossible to know whether several nuclear fragments arose from a single apoptotic cell, or several. This would have been better supported using a fluorescent probe for phosphatidyl serine, activated caspase or loss of plasma membrane integrity.

3. Borgstrom *et al.*, indicate that 'green vessels (from donor orthotopic tissue) attached to host vessels lacking GFP and blood cells circulated seamless between the contiguous vessels'- 2i: this claim is not well supported by figure. The use of shadows as a measure of vascular density is also not ideal, it would have been better demonstrated by the injection of fluorescent vascular tracers in addition also ex vivo

staining of thick sections with endothelial cell markers. For comparison, another study has recently reported imaging of endothelial cells in syngeneic tumor grafts: http://www.landesbioscience.com/journals/intravital/article/24790/?show_full_text=true .

We have read this submission. We believe that we have an appropriate level of expertise to confirm that it is of an acceptable scientific standard.

Competing Interests: No competing interests were disclosed.

Author Response 08 Aug 2013

Phil Oh, Proteogenomics Research Institute for Systems Medicine, USA

We would like to thank the reviewers for their time and comments.

1. We agree that tissue attenuation of fluorescence signal is likely and could contribute to an underestimation of tumor growth. But that is why we performed two different measurements, including one based on tumor area which is defined by the pixels reaching a minimum threshold fluorescence signal from the glowing tumor cells and thus will be much less sensitive to such attenuation. The results were very similar with both measurements. Consistent with this, these tumors tend to grow more in 2-dimensions and be a bit flattened and not so spherical in shape, in part because of the glass coverslip. Not sure that this issue is all that critical to our findings and conclusion; for the purposes of comparisons made in the paper, we used the same methods which quantified growth differences that were not particularly subtle but rather quite obvious from the captured images. Performing ex-*vivo* measurement of tumor size and weight somewhat defeats the overall purpose behind using IVM and this model system. We wish to get dynamic and continuous intravital data on the tumors at multiple scales and ultimately avoid using huge numbers of animals to get data that may only be a bit more accurate but at such a considerable cost in many different ways. There are some advantages here: because we are using tumor cells that provide the fluorescent signal specifically, we can be sure that our measurement reflects actual tumor cells and not other events that can appear to contribute to tumor size and apparent growth such as dead cells, infiltration of other cells, hemorrhage, edema, etc. Here we wish to examine effects of stroma/tissue implantation on the tumor cells themselves in-*vivo* and their proliferation. So our approach is more direct and maybe even better in many respects than simple tumor excision and weighing.

2. We have compared our definition of apoptotic cells with tunnel assays and they were very similar in their assessment of apoptosis. This was reported in reference 20. We have added a sentence in this regard in the methods citing this paper.

3. We are able to observe the blood including cells circulating through unmistakable blood vessels. The static images shown were taken from our movies. When we set up these measurements, we picked darkness thresholds that highlighted unambiguous vessels with clear blood flow. We have frequently used various fluorescent tracers which as expected provide a signal that coincides with the blood flow seen through the vessels. But this extra procedure on the mice ultimately was unwarranted for this singular purpose because it did not really augment or refine our measurement of vascularity. Again ex vivo evaluations seem contrary to noninvasive, dynamic, continuous, in vivo imaging attained here and would likely add more effort and animals but little beyond the results and conclusions

provided more efficiently through IVM. We appreciate these comments and have added further description of the vascularity measurement in the methods to provide more clarity to the reader.

Competing Interests: Author

Referee Report 14 June 2013

doi:10.5256/f1000research.1275.r1001

Hong Zhao[1], **Zhen Zhao**[2]
[1] Department of Systems Medicine and Bioengineering, Methodist Hospital Research Institute, Houston, TX, USA
[2] The Methodist Hospital Research Institute, Houston, TX, USA

The article provides a novel way to image and investigate the tumor in the original similar microenvironment. That makes it much easier to investigate the tumor characteristics related to the microenvironments.
However, there are some questions need to be clarified in the paper:
1. After the implantation of the orthotopic tissue to the dorsal skin chamber, where is the blood supply of the tissue from? Will the angiogenesis happen in the tissue like a tumor? Usually, it's a challenge to make the engrafted normal tissue to get good blood supply after the implantation. If the angiogenesis or vasculogenesis happened in the tissue, where did the vessels arise from? Were they from the host animal or just attached to the blood vessel of the host animal?
2. For the vascular parameters, I didn't notice any vascular mark methods, were they only identified by the dark space between the fluorescent tumor background? If so, will the stroma tissue in the tumor which has no fluorescent effect the counting of the blood vessels?
3. There are no units of the tumor size in the graphs of figure 1, 4, 6 and the supplement figures.

We have read this submission. We believe that we have an appropriate level of expertise to confirm that it is of an acceptable scientific standard, however we have significant reservations, as outlined above.

Competing Interests: No competing interests were disclosed.

Author Response 08 Aug 2013

Phil Oh, Proteogenomics Research Institute for Systems Medicine, USA

We appreciate these comments and have revised the text description to be clearer. We have also added a paragraph to the discussion that describes possible process differences between EO versus subcutaneous models.

1. We explicitly use donor tissue from GFP-mice so that we can definitively detect via fluorescence imaging, which parts of the tumor stroma its cells and vessels are from, the implanted tissue versus the host mouse. Moreover we also utilize tumor cells that express mCherry (red signal) for further distinction. It is clear from the figure 2 that there is ample

donor tissue represented in the stroma of these tumors. Then when we look specifically at blood vessels which are unambiguously identified by their distinct structure and the flow of blood cells through them, we readily observed that the endothelial cells lining these blood vessels fluorescence “green” from their GFP expression. To increase certainty that the cells of the vascular wall in the tumor were indeed from the implanted donor orthotopic tissue, we performed additional experiments where the tissue was donated once again from transgenic mice expressing GFP but this time the expression was more selective to cell type because it is controlled by an endothelial cell promoter. Again the vessel wall cells expressed the GFP in the tumors. Please also see manuscript text for fig. 2 which describes this directly. For example we state: “To examine the vascular endothelium more specifically, we also implanted donor tissue excised from mice expressing GFP under the endothelial cell-specific promoter TEK24. Here again, the tumor vasculature was clearly lined with GFP-expressing endothelial cells (Figure 2h) that were clearly distinct from tumor cells (Figure 2i). The green vessels attached to host vessels lacking GFP and blood cells circulated seamlessly between the contiguous vessels. The tumor stroma and neovasculature, therefore, arose from the engrafted donor tissue and successfully revascularized by attaching to the unlabeled vessels present in the host animal.” One way to think of this process is that in classic subcutaneous tumors the implanted tumor spheroid is communicating with the surrounding tissue to induce accommodations that are required for tumor growth and that include angiogenesis. It is the only supplicant for proper adaptations and maybe lacks all the means possible in a normal tissue wound repairing process. With co-implantation, the donor tissue not only communicates its similar needs but also inherently has important elements, including key cells and blood vessels, to provide in a primed state to form the surviving tissue. As a minced, wounded tissue in need of repair, it appears to be able to revascularize in part through anastomosis of its vessels with underlying blood vessels of the skin. This donor tissue can do so on its own as shown in our 2007 Nature Biotechnology article in which we state that the donor implanted tissue’s blood vessels “maintained both tissue- and species-specificity, even expressing key organ-specific biomarkers”. This donor tissue can also do so with the tumor spheroid where the two appear to work quite well together to create a functioning robust neoplastic tissue. When comparing tumors with and without the donor orthotopic tissue, it appears clear that the co-implanted stroma helps the tumor take root more quickly with faster development of functioning blood vessels leading to a significant growth advantage at least initially. It will be interesting to see how similar or not the EO and subcutaneous tumors are over time; once the subcutaneous tumors have overcome their longer lag period and achieve similar vascular densities and growth, does the incorporated orthotopic stroma contribute to sustained, long term meaningful differences between the two models?

2. We can readily differentiate the blood vessels from the non-fluorescent stroma because the blood vessels not only encompass morphologically distinct and obvious dark channels between the fluorescent tumor cells but also were identified by presence of blood cells and even actual circulating blood flow, which could easily be visualized in the movies from which the static images were made. For our measurement, we picked darkness thresholds that emphasized vessels with clear blood flow. As expected, when we have used various fluorescent tracers they provided a signal that readily coincided with the blood flow seen through the blood vessels. We appreciate these comments and have attempted to be clearer by adding more details on this to the methods section.

3. The tumor size is based on the size of the tumor on Day 1 after implantation which is normalized for each tumor to be 1. Therefore, the relative tumor growth graphs do not have any units in the Y-axis. You can see from the pictures provided that the tumors were similar but not identical in size (in part because the tumor spheroids,at the time of implantation, cannot be matched perfectly in size). Because we ultimately were interested in relative tumor growth over time between the different groups and experiments, we choose to simplify the growth curves akin to many other past published studies by this standard normalization. How we measure tumor size and growth including this normalization is described in the methods section with a brief sentence in some of the figure legends. Please note that we measured size in two ways and both gave very similar results. We appreciate these comments and have adjusted the legends and methods to be clearer.

Competing Interests: Author